Attention Enhances Synaptic Efficacy and Signal-to-Noise in Neural Circuits

Farran Briggs[1,2], **George R. Mangun**[3,4,5], and **W. Martin Usrey**[1,5,6,*]

[1]Center for Neuroscience, University of California, Davis

[2]Department of Physiology and Neurobiology, Geisel School of Medicine at Dartmouth

[3]Center for Mind and Brain, University of California, Davis

[4]Department of Psychology, University of California, Davis

[5]Department of Neurology, University of California, Davis

[6]Department of Neurobiology, Physiology and Behavior, University of California, Davis

Summary

Attention is a critical component of perception. However, the mechanisms by which attention modulates neuronal communication to guide behavior are poorly understood. To elucidate the synaptic mechanisms of attention, we developed a sensitive assay of attentional modulation of neuronal communication. In alert monkeys performing a visual spatial attention task, we probed thalamocortical communication by electrically stimulating neurons in the lateral geniculate nucleus of the thalamus while simultaneously recording shock-evoked responses from monosynaptically connected neurons in primary visual cortex. We found that attention enhances neuronal communication by (1) increasing the efficacy of presynaptic input in driving postsynaptic responses, (2) increasing synchronous responses among ensembles of postsynaptic neurons receiving independent input, and (3) decreasing redundant signals between postsynaptic neurons receiving common input. These results demonstrate that attention finely tunes neuronal communication at the synaptic level by selectively altering synaptic weights, enabling enhanced detection of salient events in the noisy sensory milieu.

Selective attention is a powerful brain mechanism that enables enhanced processing of relevant information while preventing interference from distracting events. Numerous studies in humans and animals have established that visual attention can influence sensory

*Correspondence to: wmusrey@ucdavis.edu.

information processing in visual cortex[1–7] and subcortical visual areas[8–11]. Attention directed toward stimuli within the receptive field of a neuron in visual cortex generally results in increases in neuronal firing rate[12,13] and synchrony[14,15]. More recent work indicates that visual attention can also alter the correlation structure, variability and/or response gain of neuronal activity[14,16–18]. However, the fundamental mechanisms by which visual attention alters communication in neural circuits, at the synaptic level, remain a mystery. Moreover, it is unclear how attention-mediated alterations in neuronal population activity translate into improvements in perception[19].

In order to elucidate the synaptic mechanisms of attention, we developed a sensitive electrophysiological assay of neuronal communication involving stimulation of thalamocortical neurons in the lateral geniculate nucleus (LGN) of the thalamus and simultaneous recordings from monosynaptically connected (i.e., postsynaptic) neurons in primary visual cortex (V1) of macaque monkeys performing a spatial attention task. First, we tested whether visual attention alters the efficacy of synaptic communication between the LGN and V1, defined here as the probability that presynaptic stimulation evokes a postsynaptic action potential. Second, we examined whether attention alters both signal and noise in correlated activity among ensembles of postsynaptic target neurons.

Two monkeys were trained to maintain central fixation while covertly focusing their attention on one of two drifting gratings in order to report a contrast change in the attended stimulus (Fig. 1). One of the gratings was positioned over the receptive field of recorded neurons and the other was located at an equivalent eccentricity away from the receptive fields. Trials in which attention was directed toward (attend-toward condition) and away (attend-away condition) from the receptive fields of recorded neurons were organized into blocks and cued by the color of the central fixation dot. On a random 5% of the trials the cue instruction was invalid, such that the contrast change occurred at the unattended location. Animals were rewarded for correct detection of the contrast change in validly and invalidly cued trials. Behavioral measures of spatial attention were derived by comparisons of accuracy (percentage of trials completed correctly) and reaction times on validly and invalidly cued trials. For both monkeys, accuracy was significantly greater ($p < 0.03$) and reaction times were significantly faster ($p < 0.05$; Fig. 1b) for validly versus invalidly cued trials, indicating that animals were covertly attending to the specified location.

In each animal, we implanted stimulating electrodes in the LGN (Fig. 2a) such that weak electrical shocks applied to presynaptic thalamocortical neurons evoked suprathreshold, short-, and fixed-latency monosynaptic spikes in recorded (postsynaptic) thalamocortical-recipient (TCR) neurons, located in layer 4C of V1 (Figs. 2a, b). Importantly, stimulation levels were set such that stimulation evoked a postsynaptic spike in only a fraction of trials (Supplementary Fig. 1a). We recorded visually-evoked activity in response to drifting sinusoidal gratings in order to characterize the physiological responses of all recorded TCR neurons. TCR neurons ($n = 61$) were grouped into Magnocellular-recipient (M-recipient; $n = 36$) or Parvocellular-recipient (P-recipient; $n = 25$) populations based on the stimulus contrast required to evoke a half-maximum response (Fig. 2c). M- and P-recipient neurons differed across multiple physiological parameters including orientation tuning ($p = 3 \times 10^{-7}$; Fig. 2c), the ratio of the first harmonic (f1) to mean (f0) response ($p = 1.5 \times 10^{-15}$), and

visually evoked firing rates (p = 0.04). However, shock efficacies (Supplementary Fig. 1a), spontaneous firing rates, and shock-evoked postsynaptic-response latencies (Fig. 2b) did not vary significantly across the M- and P-recipient populations, consistent with previous reports[20].

Once TCR neurons were physiologically characterized, we then recorded both visually-evoked and shock-evoked neuronal responses while animals performed the attention task. On a subset of attention trials (70%), a single shock was delivered to the LGN between 1,000 and 1,200 msec following the onset of grating presentation and prior to the contrast change. Electrical stimulation did not affect performance, as there was not a significant difference in the animals' ability to complete shock and non-shock trials in the attend-toward or attend-away conditions (p > 0.5). When we compared thalamocortical synaptic efficacy (percent of presynaptic shocks that evoked a postsynaptic spike) as a function of attention, we observed a highly significant increase in synaptic efficacy when covert spatial attention was directed toward the receptive fields of recorded TCR neurons compared to when attention was directed away from TCR receptive fields (p = 1×10^{-7}; Fig. 2d). Attentional modulation of synaptic efficacy was significant for both M- and P-recipient neuronal populations (p = 6×10^{-5} and p = 9×10^{-4}, respectively). For the attend-away trials, it is interesting to note that the number of spikes occurring within the time window corresponding to the postsynaptic response latency did not differ between shock and non-shock trials (Supplementary Fig. 1b), despite the fact that shock strength was set to be effective in non-attention conditions. This finding is consistent with the view that attention may also have a suppressive influence on synaptic efficacy when directed away from a neuron's receptive field.

The robust attentional enhancement of thalamocortical synaptic efficacy, indexed by the positive shift in shock-evoked spike efficacy across attention conditions (Fig. 2e), contrasts with a modest attention-mediated increase in neuronal firing rate (Fig. 2f; statistically significant for M-recipient [p = 0.01], but not P-recipient [p > 0.1] neurons). Interestingly, this modest increase in firing rate across attention conditions was only evident for later time periods between stimulus onset and the earliest opportunity for contrast change (850–1,200 msec and 1,000–1,200 msec), and was not evident over earlier or broader time periods (0–1,200 msec or 600–1,200 msec; p = 0.9; Supplementary Fig. 1c), consistent with prior studies showing weak or no attentional modulation of firing rate in V1[6,21–24]. Further analysis also demonstrated that there was no relationship between the magnitude of attention effects on firing rate and the influence of attention on the efficacy of thalamocortical communication (Supplementary Fig. 1d). These results suggest that (1) attentional modulation of synaptic efficacy in thalamocortical circuits is not merely due to simple gain or firing-threshold changes in LGN or TCR neurons; and (2) thalamocortical visual pathways may utilize a different (synaptic-level) mechanism to propagate attentional signals compared to higher visual areas, where attentional modulation can be indexed by changes in neuronal firing rates.

We further explored the temporal precision of attentional modulation of synaptic efficacy in thalamocortical circuits by examining spiking activity over a 10-msec window surrounding the time of the shock-evoked postsynaptic spike. Figures 3a and 3b illustrate the population

average time-course of differential spiking activity (attend-toward – attend-away) surrounding the shock-evoked postsynaptic spike (defined as time = 0) for M- and P-recipient neurons, respectively (see Supplementary Fig. 2a for separate time-course plots corresponding to each attention condition). In both cases, spiking activity rises above two standard deviations of the mean activity for 2–3 msec, indicating that attention causes an increase in the number of synaptically evoked spikes during a limited time window. Interestingly, about 40% of TCR neurons (42% of M-recipient neurons; 40% of P-recipient neurons) displayed a prominent dip in spiking activity just prior to the evoked spike (Figs. 3a, b; Supplementary Figs. 2a, b), suggesting that fast feedforward inhibition, likely via local interneurons, may suppress spiking activity just prior to the occurrence of the postsynaptically evoked spike. Accordingly, we found that TCR sub-populations with fast feedforward inhibition displayed less jitter in the timing of their shock-evoked postsynaptic spikes (response profile = 1.75 msec for Dip neurons versus 2.75 msec for No-dip neurons; Fig. 3c). These results suggest that feedforward inhibition sharpens postsynaptic spike-timing precision by about 1 msec. The presence of dips illustrates that attentional modulation in our sample of V1 neurons was often dynamic, including phases of reduced spiking as well as phases of increased spiking. These dynamics could help explain why attentional modulation did not yield a larger increase in overall firing rate.

Having established that attention alters the efficacy of synaptic communication in neural circuits with fine temporal precision, we next set out to determine whether attention differentially affects the processing of signal and noise in thalamocortical circuits. Prior studies have provided evidence to suggest that attention may alter neuronal activity by increasing signal or reducing noise in firing rate fluctuations[20,22]. We assessed whether attention could both boost signal and reduce noise in the same circuit by examining the effects of attention on the occurrence of synchronized spikes between pairs of simultaneously recorded TCR neurons. In some circumstances, synchronized spiking may boost signal detection by more effectively driving downstream targets[25,26], while in other cases, synchronized spiking may confound decoding by downstream target neurons through introduction of noise[27]. Using a multi-electrode recording array, we recorded from 71 pairs of simultaneously recorded TCR neurons that fired synchronized spikes in response to electrical stimulation in the LGN. Our criteria for identifying synchronous postsynaptic spikes were strict: in any given trial, synchronous spikes needed to occur at the specified shock-evoked postsynaptic spike latencies for each TCR neuron in the pair. For each pair, we calculated the percentage of trials in which synchronous spikes were evoked in response to electrical stimulation in the attend-toward versus attend-away conditions. Results from this analysis were clear – attention significantly increased the percentage of synchronous spikes across our sample of TCR pairs (Figs. 4a, b; $p = 3.6 \times 10^{-8}$). This effect was present for M-M, P-P, and M-P pairs in our sample ($p < 0.04$; indicated in Figs. 4a, b with black, green, and grey symbols, respectively), suggesting that attentional modulation of spike synchrony is consistent across thalamocortical circuits.

Synchronized spiking between pairs of TCR neurons could arise from two sources: (1) the simultaneous arrival of spikes traveling in *independent* channels of communication (e.g., different LGN axons); and (2) the simultaneous arrival of spikes traveling in a *common*

channel (e.g., one LGN axon) with divergence. Although both mechanisms will propagate signal (stimulus evoked) and noise spikes to their postsynaptic targets, randomly generated noise spikes are less likely to occur simultaneously between independent LGN axons than between the branches of common input LGN axons. Consequently, attention could increase the ratio of signal-to-noise in thalamocortical circuits by increasing the strength of spikes arriving from independent channels, and also by reducing the strength of spikes arriving from common-input channels. To determine whether pairs of TCR neurons in our sample received common LGN input, we calculated shuffle-corrected cross-correlograms from TCR neuronal responses to drifting sinusoidal gratings. For 25 TCR pairs, cross-correlograms contained a single, narrow (<3 msec, full width at half height) peak centered at time zero, indicating that the two neurons frequently fired synchronous spikes in response to common feedforward input (Fig. 4c). TCR pairs in our sample with zero-centered cross-correlogram peaks had overlapping receptive fields, consistent with prior studies of correlation patterns exhibited by visual neurons with common feedforward input[26]. Most recorded TCR pairs consisted of two M-recipient neurons or two P-recipient neurons, consistent with the anatomical segregation of magnocellular and parvocellular inputs to V1. However, we also encountered pairs of mixed M- and P-recipient neurons.

For TCR pairs receiving common input, we calculated the percentage of synchronous spikes (i.e., the percentage of spikes contained in the cross-correlogram peak) when attention was directed towards and away from the cells' receptive fields. Results of this analysis revealed that attention decreased synchronous spikes from common input by ∼10% (see Supplementary Methods). Accordingly, the distribution of differential cross-correlogram peak height (attend-toward – attend-away) was shifted significantly to the left of zero (p = 0.004), indicating that attention decreased synchronous responses to common input (Fig. 4d). These results suggest that attention may decrease noise in thalamocortical communication by reducing the amount of synchronous spikes arising from common feedforward input.

As a final analysis, we explored whether attention differentially modulated synchronous spiking in pairs of TCR neurons receiving input from independent sources (i.e., TCR pairs with flat cross-correlograms) compared to TCR pairs that received input from common sources (i.e., TCR pairs with narrow, zero-centered cross-correlogram peaks). More specifically, we determined whether *measured* percentages of synchronous spikes differed from *predicted* percentages based on the product of the evoked postsynaptic spike probabilities measured for each TCR neuron in the pair (Fig. 4e). For TCR neurons receiving common input, the percentage of measured synchronous spikes was not significantly different from the prediction (p = 0.3), and there was no effect of attention on this relationship. However, for TCR pairs receiving independent input, there was a significant difference between actual and predicted synchronous spikes, and attention had a significant effect on the relationship between measured and predicted values (p = 0.02). These results suggest that attention differentially regulates synchronized inputs emerging from independent and common sources. Accordingly, attention boosts signal transmission by enhancing responses to synchronous inputs from independent sources and reduces noise transmission by reducing responses to synchronous inputs from common input sources.

Based on our data, attention may boost signal-to-noise ratios on average by approximately 20% (see Supplementary Materials). This finding has significant implications for understanding the mechanisms by which neural networks optimally encode sensory information in the face of potentially noisy correlations resulting from anatomical wiring constraints[27].

Taken together, the results of this study provide multiple insights into the mechanisms by which attention alters neuronal communication. First, attention modulates signal transmission by enhancing synaptic efficacy. This finding represents the first evidence that attention acts at the synaptic level. Second, attention modulates afferent signal transmission with fine temporal precision. Third, attention serves to increase the ratio of signal-to-noise in neural circuits by simultaneously enhancing the transmission of signal and reducing the transmission of noise. These results strongly suggest that attention modulates synaptic inputs in a highly selective manner such that inputs carrying salient sensory information (via independent channels) are enhanced and inputs carrying potentially redundant information (via common channels) are suppressed. Each of these results has significant implications toward understanding attentional modulation of sensory information processing.

Attentional modulation of synaptic efficacy in thalamocortical circuits was robust and displayed temporal precision. Attention-related improvements in spike-timing precision in V1 resulted in part from fast disynaptic feedforward inhibition. Interestingly, the temporal precision of attentional modulation of V1 activity did not strongly correlate with more global changes in firing rate (represented by an attention index calculated from peri-stimulus spiking activity). This lack of correspondence suggests that attention alters brain activity via multiple mechanisms including more global alterations in neuronal firing rate, as well as finer-scale dynamic alterations in synaptic communication operating at the level of individual neural circuits. Moreover, our results support the notion that attentional modulations involving fine-scale dynamics may not manifest in more global alterations in neuronal firing rate. At the local circuit level, this effect may serve to enhance spatial and temporal precision, but at the more global level, these effects may average out. In V1 (and other sensory cortices), attention may utilize fine-scale dynamics in order to accommodate depressing synapses, a known property of thalamocortical afferents[28]. Although beyond the scope of the current study, it would be interesting to know whether or not attention affects synaptic weights in higher visual cortical areas and, if so, whether or not the effects of attention on synaptic weights underlie the influence of attention on neuronal firing rate dynamics.

Our data support the notion that attention directly enhances sensory information processing by increasing the ratio of signal-to-noise in neural circuit communication. Simultaneous signal enhancement and noise reduction in the same neural circuit suggests that attention modulates correlated synaptic activity in a highly selective manner. Select synaptic connections originating from independent inputs and carrying feature-specific information about a sensory stimulus are more strongly weighted with attention, leading to better processing of salient stimulus features by downstream neurons. Synaptic connections originating from common inputs are weighted less with attention such that false positives are less likely to be communicated to downstream decoding neurons. Such asymmetric synaptic

weighting with attention hints at a presynaptic locus for modulation, as a postsynaptic locus, such as altering the membrane potential threshold of cortical recipient neurons, would be difficult to reconcile with asymmetric synaptic weights. Along these lines, the finding that attention does not increase the overall firing rate of cortical neurons that receive direct LGN input indicates that the measured changes in thalamocortical communication are unlikely to be due to a generalized depolarization among target neurons with attention. Although determining the structural basis for presynaptic modulation lies beyond the scope of the current study, one possible candidate is differential modulation by acetylcholine. Acetylcholine has been implicated in attention effects in V1[29], and a particular class of cholinergic receptors are localized to the presynaptic terminals of LGN axons that innervate cortical layer 4C neurons[30]. These cholinergic synapses could therefore provide a route for attention to selectively alter synaptic weights.

Feedforward subcortical-cortical and cortico-cortical connections often must convey information with speed and precision, but anatomical wiring constraints on these connections can introduce unreliable information. Here we demonstrate that attention alters synaptic communication in a dynamic and highly selective manner that could be uniquely adapted for signal transmission in sensory cortex. Specifically, attention selectively enhances inputs carrying salient sensory information while simultaneously suppressing inputs carrying potentially redundant information. These findings suggest that attention could represent a critical mechanism by which anatomical wiring limitations are overcome in order to optimize communication across neural circuits, thereby permitting the most behaviorally relevant information to influence perception and performance.

Methods

Two adult female macaque monkeys (*Macacca mulatta*) were used for this study. All of the procedures performed as a part of this study conformed to the guidelines set forth by the NIH and were approved by the Institutional Animal Care and Use Committee at the University of California, Davis.

Surgical Preparation

All surgical procedures have been described in detail previously[31,32]. Under full surgical anesthesia, two craniotomies were made to allow recording access to the LGN and to the parafoveal opercular region of V1. Two recording cylinders were placed encircling the craniotomies and incased in an implant of bone cement. Head restraint posts were also attached to cranial implants. Following recovery from surgery, cylinders were flushed with sterile saline plus Betadine or chlorhexidine at least 3 times per week. Weekly, 5-fluorouracil treatment, and occasional dura scrapes, were performed in order to maintain thin and healthy dura for ease of electrode penetration.

Visual Stimulation

Visual stimuli were generated using a VSG/5 system (Cambridge Research Systems, Rochester, UK). Stimuli were presented on a gamma-calibrated Sony monitor (Tokyo, Japan) placed 700 mm in front of animals' eyes. The refresh rate of the monitor was 140 Hz

and the mean luminance was 38 cd/m^2. The monitor was the sole source of illumination in the room with the animal. All stimuli were presented under binocular viewing conditions.

Behavioral Training

Animals were trained to perform fixation and contrast-change detection tasks for juice rewards using standard operant conditioning. Eye position was monitored by an infrared video eye tracker (Applied Science Laboratories, Bedford, MA) with a refresh rate of 240 Hz. If animals' eye position deviated by more than 0.35° at any point during a task trial, the trial was aborted. Fixation tasks required animals to maintain central fixation on a dot while drifting gratings were placed within the receptive fields of recorded neurons in order to measure neuronal visual physiology. For fixation tasks, trials were interleaved with a minimum 1-second period during which the monitor was mean luminance grey and animals were allowed to freely move their eyes.

Attention Task

Animals were trained to detect a contrast change in one of two gratings with a movement of a joystick such that visual fixation could be maintained throughout the entire duration of the trial, including the answer window. Animals were instructed to attend either to a drifting sinusoidal grating presented within (attend-toward condition) or an identical grating presented outside (attend-away condition) the receptive fields of the recorded neurons (Fig. 1a). The two gratings were identical and set to the orientation and spatial-frequency preference of the recorded neurons, and were always equal-distant from the central fixation dot. Attention trials were run in blocks of 10 trials of each attention condition (attend-toward or attend-away) and the color of the central fixation dot cued the animals where to allocate their attention. Trials progressed as follows. Trials were interleaved with a minimum 1,000-msec period, during which the monitor was mean luminance grey and the animals were allowed to freely move their eyes, after which the monkey initiated a new trial by moving a joystick from the center position to a side position (left or right of center). Animals were required to maintain the joystick in the side position throughout the duration of the trial until the answer period – premature joystick movements caused trials to abort. Upon initial movement of the joystick to the side, a central fixation dot was displayed, to which animals directed their gaze. Five hundred msec following the onset of central fixation, two gratings appeared on the monitor, one inside and one outside the receptive field of recorded neurons. The two gratings were presented for a variable amount of time between 1,200 and 2,500 msec as determined on a trial-by-trial basis according to a hazard function with a mean at 1,700 msec. Following the period of visual stimulation by drifting gratings as determined by the hazard function, one of the two gratings increased in contrast by 10%. Both gratings remained on the monitor during a 500 msec answer window in which animals signaled detection of the contrast change by moving the joystick to the original central position. Only correct detection of the contrast change, indicated by a correct joystick movement, while also maintaining central gaze fixation throughout the answer period, was rewarded with juice. Trained animals typically performed at or above 70% correct, discounting aborted trials. Trials were aborted when animals moved their eyes by more than 0.35° during any portion of the trial or made a joystick movement prior to the contrast change. We found no significant differences in the proportion of aborted trials across attention conditions or

across shock and non-shock trials ($p > 0.5$). Importantly, prior to the contrast change, visual stimulation was equal across attention conditions such that the only variable differing across conditions was the location to which the animal directed covert spatial attention.

Across blocks of trials, 95% of total trials were validly cued, wherein the contrast change occurred at the attended location signified by the color of the fixation dot. In the remaining 5% of trials, the fixation dot color cue was invalid and the contrast change occurred at the unattended location. Reaction times were measured as the time between the contrast change and movement of the joystick back to the central position. For each animal, reaction times were compared across validly and invalidly cued trials. Reaction time data were computed for all sessions including at least 50 correct trials in each attention condition (attend-toward and attend-away). Reaction time values were: Monkey B (MB): RT-Valid = 363±5 msec, RT-Invalid = 401±14 msec (Monkey B, $p = 0.006$); Monkey O (MO): RT-Valid = 387±7 msec, RT-Invalid = 435±21 msec (Monkey O, $p = 0.046$). Additionally, both monkeys correctly detected grating contrast changes significantly more often in validly compared to invalidly cued trials ($p < 0.03$).

Electrical Stimulation

As described in detail previously[31,32], stimulating electrodes were semi-chronically implanted within parafoveal regions of the LGN. Stimulating electrodes were placed in precise retinotopic alignment with recording electrodes in V1 such that receptive fields of neurons at each location were within less than 2° of one another in visual space. Single platinum/iridium stimulating electrodes (FHC, Bowdoin, ME) with < 1 mm of tip exposure were placed within the LGN such that both magnocellular and parvocellular thalamocortical neuronal populations were activated. Placement of stimulating electrodes was guided and verified by recording visual responses from LGN neurons during and following implantation. Stimulation was generated by an AM Systems isolated pulse stimulator (Carlsborg, WA) and included a single, brief (0.2 msec), biphasic current pulse (∼10–200 µA) delivered once every 5 seconds during collision testing (described below) and once per shock trial in the attention task (described below).

In order to locate putative thalamocortical-recipient (TCR) neurons, V1 recording electrodes were slowly advanced while shocks were delivered at regular intervals (every 5 seconds). TCR neurons were identified by the presence of short-latency (<6 msec), feedforward postsynaptic spikes in both collision and non-collision modes of stimulation, as described in detail previously [31,32]. Shock-evoked postsynaptic spike latencies were calculated as the time between the shock in the LGN and the postsynaptic spike. M- and P-recipient neurons did not differ in their postsynaptic spike latencies (Fig. 2b; $p = 0.5$).

Collision testing was performed in order to distinguish whether or not cortical neurons were activated by the arrival of orthodromically or antidromically propagated spikes following electrical stimulation. Collision tests were performed while the animals performed fixation tasks, or when mean luminance grey was displayed on the monitor and animals were allowed to move their eyes freely. Shock current was set such that shocks evoked spikes ∼35% of the time, on average, regardless of the behavioral condition or stimulus display. It was important to titrate the shock current for each individual TCR neuron such that shock-

evoked postsynaptic spikes occurred on a fraction of trials in order to avoid floor or ceiling effects in the attention experiment. In 76 of 80 recording sessions, shock strength was held constant across collision and attention testing conditions; in 4 sessions, shock strength was decreased for attention trials relative to collision trials.

Electrical Stimulation During Attention Task

In 70% of attention trials, a single shock (parameters as above, current set per TCR neuron) was delivered between 1,000 and 1,200 msec following the onset of the two drifting sinusoidal stimuli and prior to the contrast change. Shocks occurred at the same time in the stimulus cycle for both attend-toward and attend-away trials. The precise timing of the shock was set to match the neuron's peak response to the periodic stimulus. In this way, electrical stimulation occurred while the recorded neuron was excited (rather than suppressed) by the visual stimulus. Shocks were delivered toward the end of the visual stimulation period because animals' reaction times systematically decreased with increasing visual stimulation duration, suggesting that animals' exerted greater attention toward the end of each trial (data not shown).

The efficacy of shocks in evoking postsynaptic spikes was determined for each TCR neuron based on all shock trials in the attention task, including attend-toward and attend-away trials (Supplementary Fig. 1a). M- and P-recipient neurons did not differ in their shock-evoked spike efficacies (Supplementary Fig. 1a; $p = 0.1$).

Animals did not make voluntary or involuntary eye movements in response to electrical stimulation of the LGN (which would have resulted in aborted trials since shocks occurred prior to grating contrast changes), and electrical stimulation did not affect performance on the attention task. Because electrical stimulation parameters were reduced such that the average efficacy of shock-evoked postsynaptic spikes was ~35%, and because the same proportion of trials included shocks in both attention conditions, it is unlikely that shocks induced visual percepts that interfered with animals' behavior or changes in neuronal responses across attention conditions.

Electrophysiological Recordings

Recordings from V1 neurons were made using either single platinum-in-glass electrodes (Alpha Omega, Israel) or a Mini Matrix multi-electrode array of 5 quartz-platinum/tungsten electrodes (Thomas Recording, Giessen, Germany). Spiking data were amplified and recorded by a PC equipped with a Power 1401 acquisition system and Spike2 software package (Cambridge Electronic Design, Cambridge, UK). For each recording session, the first step was identification of putative TCR neurons (described above). The second step involved characterizing the visual physiology of recorded neurons. This was accomplished by presenting drifting sinusoidal gratings varying in orientation, contrast, spatial frequency, or size within the center of the receptive field while animals performed the fixation task. Gratings were presented for 1–2 seconds per trial, and trials were repeated at least 2 times. In order to generate response functions for orientation (0–360°), contrast (0–100%), spatial frequency (0.2–4 cycles/°), and size (0.2–10°), individual parameters were increased in 10–15 step increments while all other parameters were held constant. Once optimal stimulus

parameters were determined, optimal gratings were presented for 2 seconds per trial in order to determine the precise time (the time of peak response to the periodic stimulus) to deliver electrical stimulation (see above). Finally, neurons were recorded while animals performed the attention task. Gratings drifted at 4 Hz and were of optimal orientation, spatial frequency, and ~2–4 times the size of the receptive field to accommodate small shifts in eye position (<0.35°). Grating contrast was 70% for putative P-recipient neurons and between 10 and 25% for putative M-recipient neurons. For recording sessions where multiple neurons were simultaneously recorded using the multi-electrode array, gratings parameters were set to stimulate the maximum number of cells as optimally as possible and grating sizes were set to cover the receptive fields of all recorded neurons (never > 2° since receptive field locations were always highly overlapping). If putative M- and P-recipient neurons were recorded simultaneously, grating contrast was set to an intermediate value ~40–50%. For the contrast change detection portion of the attention task, contrast always increased by 10% of the starting contrast.

Data Analyses

All recorded spikes were sorted offline using Principle Components Analysis (Spike2 software standard algorithms). Recordings were made from 161 neurons in V1, of which 61 neurons were identified as TCR neurons based on responses during collision testing. Of these 61 TCR neurons, 22 were recorded with single electrodes (15 from Monkey B, 7 from Monkey O), and 39 were recorded with the multi-electrode array (30 from Monkey B, 9 from Monkey O). Twenty-nine additional neurons were classified as putative TCR neurons in multi-electrode recordings (21 from Monkey B, 8 from Monkey O) based on shock-evoked responses during the attention task. For these neurons, shock-evoked postsynaptic responses were not consistent during collision testing because the shock current was set to accommodate the activity of a different, identified neighboring TCR in the same recording session. However, during the attention task, shocks systematically evoked postsynaptic spikes at fixed latencies consistent with monosynaptic responses. Because TCR neurons and putative TCR neurons did not differ significantly from each other in their percentages of synchronous evoked spikes in attend-toward or attend-away conditions (p > 0.2), both groups of neurons were included in subsequent analyses of synchronized and correlated spiking across attention conditions (see below). Receptive fields for all recorded TCR neurons were located in the lower left visual hemifield at parafoveal eccentricities. There were no differences in physiological response properties or attentional modulation of neurons recorded in the two monkeys, and thus, neurophysiological data from both monkeys were combined for all analyses.

TCR neurons were designated as M- or P-recipient neurons by their C50 values (contrast to evoke a half-maximum response) measured from exponential fits to their contrast-response functions. M-recipient neurons (n = 36) were classified as neurons with C50 values less than 30% and P-recipient neurons (n = 25) were classified by C50 values greater than 30%. All neurons were classified as simple or complex cells based on the ratio of the first Fourier coefficient (f1) to mean (f0) response where simple cells have f1/f0 > 1 and complex cells have f1/f0 < 1[33]. Mean f1-to-f0 ratios were: M-recipient neurons: 0.4±0.04; P-recipient neurons: 1.2±0.06 (p = 1.5×10^{-15}). Subsequent analyses of firing rates for visual

physiological characterizations and attention index calculations were performed on each neuron's f1 (simple cells) or mean (complex cells) response. Orientation tuning bandwidth was determined by calculating the peak half-width at half-height of Gaussian fits to individual orientation tuning curves.

Firing rates were measured during inter-trial-intervals and during fixation prior to the presentation of gratings during the attention task. There were no significant differences between M- and P-recipient neurons or across attention conditions for these firing rate measurements ($p > 0.7$). Firing rates were also measured during visual stimulus presentation prior to the contrast change during attention trials. M-recipient neurons had significantly higher firing rates during this period ($p = 0.04$; mean = 246 ± 19 spikes/sec) compared to P-recipient neurons (mean = 185 ± 23 spikes/sec), but firing rates assessed over this period for both M- and P-recipient neurons did not differ between attend-toward and attend-away conditions ($p = 0.9$).

For all analyses involving percentages of shock-evoked spikes, trials were sorted according to whether or not a spike occurred at the specific and fixed postsynaptic spike latency for each individual TCR neuron. Shock-evoked postsynaptic spikes were tabulated from a 2-msec wide window aligned by the spike latency. The proportions of shocks that evoked a postsynaptic spike in each attention condition were determined for each TCR neuron. We also calculated the proportion of non-shock trials in which a spike occurred at the same latency for each attention condition to allow for a comparison between the number of spikes within the latency window with and without electrical stimulation (Supplementary Fig. 1b). As expected, shocks elicited significantly more spikes at the postsynaptic response latency compared to the number of spikes that occurred in the same time window during non-shock trials for the attend-toward condition ($p = 0.003$). However, there were no differences in the number of spikes occurring at the postsynaptic response latency between non-shock and shock trials for the attend-away condition.

For each TCR neuron, an attention index value was calculated as the difference (attend-toward – attend-away) divided by the sum (attend-toward + attend-away) of average spiking activity over a specified duration of visual stimulation and always prior to the earliest opportunity for contrast change in attention trials. Importantly, AI value calculations always included the time windows corresponding to the shock and shock-evoked postsynaptic responses (which occurred between 1,000 and 1,200 msec in all trials). We calculated AI values over long and short durations of visual stimulation: 0–1,200 msec; 600–1,200 msec; 850–1,200 msec; and 1,000–1,200 msec following the onset of grating stimulation. When we calculated AI values based on firing rate over long durations (0–1,200 msec and 600–1,200 msec following grating presentation), we observed no changes in AI across attention conditions (Supplementary Fig. 1c). When we calculated AI over short durations (850–1,200 msec and 1,000–1,200 msec), we observed very small shifts in AI for M-recipient neurons only. We compared AI values for short durations to spike efficacy values and observed no relationship between overall changes in firing rate with attention and changes in spiking efficacy with attention (Supplementary Fig. 1d).

In order to examine the influence of attention on the temporal precision of thalamocortical communication across our sample of recorded TCR neurons, we aligned each TCR's ongoing spiking responses before and after individual shocks such that time = 0 corresponded to the time when the TCR neuron was expected to produce a shock-evoked postsynaptic response (determined from the shock-evoked postsynaptic latency). This allowed for averaging of spiking activity (or differential spiking activity: activity in attend-toward trials minus activity in attend-away trials) across M- and P-recipient neurons with different feedforward spike latencies. In order to assess the jitter in postsynaptic spike timing across attention conditions, we also plotted time courses surrounding shocks separately for each attention condition (Supplementary Fig. 2a). For illustrations of differential spiking activity for M- and P-recipient neurons, we reported two times the standard deviation of average spiking activity prior to the shock. In all cases, error ranges were reported as standard error of the mean. We also separated M- and P-recipient neurons into two sub-populations based on the presence of a negative dip in spiking activity just prior to the postsynaptic spike (15 M-recipient and 10 P-recipient neurons displayed negative dips). TCR neurons were classified as "Dip" neurons when differential spike count values at −2 or −1 msec time points were less than two times the standard deviation of the mean activity prior to the shock. There was no relationship between spike latency and whether or not a neuron displayed a dip (p = 0.8). Moreover, across the sample of "Dip" neurons, there was a range of spike latencies, including latencies longer than the period of the dip, indicating that dips were not systematically a consequence of the shock-induced stimulus artifact obscuring our ability to detect spikes. Supplementary Figures 2a and b illustrate spiking activity surrounding the postsynaptic spike for Dip and No-Dip TCR sub-populations (with M- and P-recipient groups plotted separately in Supplementary Figure 2b). We fit Gaussian equations to positive peaks (corresponding to shock-evoked postsynaptic spikes) for Dip and No-Dip population average curves in order to calculate the width at half-height values for each fit.

During 18 sessions (13 from Monkey B, 5 from Monkey O) we utilized a 5-channel multi-electrode array with independently movable microelectrodes (Thomas Recording Mini-Matrix system) and recorded from 39 TCR neurons and 29 putative TCR neurons (see above). In 3 of the 18 sessions we recorded from a single TCR neuron. Sessions with paired recordings were as follows: 3 sessions with 1 pair, 1 session with 2 pairs, 2 sessions with 3 pairs, 1 session with 4 pairs, 1 session with 5 pairs, 2 sessions with 6 pairs, 3 sessions with 7 pairs, and 2 sessions with 9 pairs (total = 71 pairs across 15 sessions; mean = 3.3 cells recorded per session). Of 71 total pairs, 25 received common input (i.e. cross-correlograms contained a central narrow peak at time = 0) and 46 received independent input. We examined all 50 of the possible common input pairings (in both directions) and utilized 45 pairings for the analysis of attentional modulation of correlated inputs for pairs receiving common presynaptic input (5 pairings were excluded for lack of sufficient spikes and/or noisy correlograms). To determine whether recording sessions with several pairs did not systematically bias the results, we compared attentional modulation of correlated spikes across recording sessions with greater than 2 pairings and found no differences in attentional modulation of correlated spikes across sessions (p > 0.05). We recorded a total of 48 M-M pairs (21 received common input, 27 received independent input); a total of 11 P-P pairs (2

received common input, 9 received independent input); and a total of 12 M-P pairs (2 received common input, 10 received independent input).

We calculated the probability that shocks would evoke synchronous spikes in both TCR neurons across attention conditions. Importantly, our criteria for defining synchronous spikes were strict. Trials with synchronous spikes were those where each TCR neuron fired a shock-evoked postsynaptic spike at its identified postsynaptic spike latency (n=71 pairs).

Cross-correlation analysis was used to determine whether pairs of TCR neurons received input from independent (i.e., separate) LGN axons or input from common LGN axons with presumed anatomical divergence. Cross correlations were calculated on a trial-by-trial basis for each of the 71 TCR pairings using spiking data from the 600–1,200 msec period of visual stimulation. Shuffled cross correlations were also calculated for each pairing by correlating spikes from neuron A shifted by one stimulus cycle (250 msec) compared to those of neuron B. For each trial, the shuffled correlogram was subtracted from the original correlogram. By employing trial-specific shuffle corrections, we eliminated spike correlations emerging from slow co-variations in neuronal firing rate[34] and co-activation from a common visual stimulus (stimulus-dependent correlations). Shuffle-subtracted correlograms were reported as average percentages of total spikes for each attention condition.

Of 71 pairs of simultaneously recorded TCR neurons, 25 pairs (17 from Monkey B, 8 from Monkey O) displayed narrow peaks (<3 msec) in their cross correlograms, centered at time zero, indicating the pair received common presynaptic input, presumably from feedforward axons with branches that contacted both neurons. In addition to M-M (n = 21) and P-P pairs (n = 2), we also encountered mixed M-P pairs (n = 2) receiving common input. Neurons in mixed M-P-recipient pairs were located within close proximity to one another in cortical depth (within 75 μm), and tended to display similar contrast sensitivity and/or orientation selectivity, suggesting that neurons in these mixed pairs were both located near the laminar border between layers 4Cα and 4Cβ.

For the analysis of attentional modulation of TCR pairs receiving common input, we calculated the difference in peak area, measured in 3 bins of 1 msec width centered at time = 0, between shuffle-corrected cross-correlograms in each attention condition. Cross-correlogram peak heights in each attentional condition corresponded to roughly 3% of total spikes (Fig. 4c) and the average attention-mediated reduction in peak height across all cells was −0.3±0.2% suggesting that attention caused a 10% reduction in correlated spiking resulting from divergent input from a common presynaptic source.

In order to compare actual measured percentages of synchronous shock-evoked postsynaptic spikes to predicted percentages, we compared the measured incidences of synchronous spikes (as described above) with the product of each individual neuron's probability of firing a postsynaptic spike in response to the shock (e.g. Fig. 2d). We then calculated the difference (actual – predicted) in the occurrence of synchronous spikes for common input TCR pairs and independent-input TCR pairs across attention conditions.

Approximation of overall attentional modulation of signal-to-noise ratio was calculated as: (change in % signal) / (change in % noise) which translates to: (1 + average % increase in shock-evoked synchronized spikes) / (1 - average % decrease in synchronized spikes in cross-correlogram peaks). Average % increase in shock-evoked synchronized spikes = 8% and average % decrease in synchronized spikes in cross-correlogram peaks = 10% for the population of recorded TCR pairs (see above).

Statistics

Parametric or non-parametric comparisons tests (t-test or ranksum test, respectively) were used for all two-sample comparisons depending on the distribution normality of the samples tested. In order to test for distribution normality, one-sample Kolmogorov-Smirnov tests were employed. In order to examine whether any given distribution of data differed from an equivalent normal distribution, the sample distribution was compared to a normal distribution with the same standard deviation as the sample. Accordingly, the Kolmogorov-Smirnov test compared a sample distribution to a hypothesized continuous distribution defined by the same range and variance parameters as the sample.

Supplementary Material

Refer to Web version on PubMed Central for supplementary material.

Acknowledgments

References

1. Van Voorhis S, Hillyard SA. Visual evoked potentials and selective attention to points in space. Perception and Psychophysics. 1977; 22:54–62.

2. Moran J, Desimone R. Selective Attention Gates Visual Processing in the Extrastriate Cortex. Science. 1985; 229:782–784. [PubMed: 4023713]

3. Heinze HJ, et al. Combined spatial and temporal imaging of brain activity during visual selective attention in humans. Nature. 1994; 372:543–546. [PubMed: 7990926]

4. Ito M, Gilbert CD. Attention modulates contextual influences in the primary visual cortex of alert monkeys. Neuron. 1999; 22:593–604. [PubMed: 10197538]

5. Kelly SP, Gomez-Ramirez M, Foxe JJ. Spatial attention modulates initial afferent activity in human primary visual cortex. Cerebral Cortex. 2008; 18:2629–2636. [PubMed: 18321874]

6. McAdams CJ, Reid RC. Attention modulates the responses of simple cells in monkey primary visual cortex. J. Neuroscience. 2005; 25:11023–11033. [PubMed: 16306415]

7. Thiele A, Pooresmaeili A, Delicato LS, Herrero JL, Roelfsema PR. Additive effects of attention and stimulus contrast in primary visual cortex. Cerebral Cortex. 2009; 19:2970–2981. [PubMed: 19372142]

8. Vanduffel W, Tootell RB, Orban GA. Attention-dependent suppression of metabolic activity in the early stages of the macaque visual system. Cereb Cortex. 2000; 10:109–126. [PubMed: 10667980]

9. O'Connor DH, Fukui MM, Pinsk MA, Kastner S. Attention modulates responses in the human lateral geniculate nucleus. Nat Neurosci. 2002; 5:1203–1209. [PubMed: 12379861]

10. McAlonan K, Cavanaugh J, Wurtz RH. Guarding the gateway to cortex with attention in visual thalamus. Nature. 2008; 456:391–394. [PubMed: 18849967]

11. Schneider KA, Kastner S. Effects of sustained spatial attention in the human lateral geniculate nucleus and superior colliculus. J. Neuroscience. 2009; 29:1784–1795. [PubMed: 19211885]

12. Spitzer H, Desimone R, Moran J. Increased attention enhances both behavioral and neuronal performance. Science. 1988; 240:338–340. [PubMed: 3353728]

13. McAdams CJ, Maunsell JH. Attention to both space and feature modulates neuronal responses in macaque area V4. J Neurophysiol. 2000; 83:1751–1755. [PubMed: 10712494]

14. Fries P, Reynolds JH, Rorie AE, Desimone R. Modulation of oscillatory neuronal synchronization by selective visual attention. Science. 2001; 291:1560–1563. [PubMed: 11222864]

15. Lakatos P, Karmos G, Mehta AD, Ulbert I, Schroeder CE. Entrainment of neuronal oscillations as a mechanism of attentional selection. Science. 2008; 320:110–113. [PubMed: 18388295]

16. Cohen MR, Maunsell JH. Attention improves performance primarily by reducing interneuronal correlations. Nat Neurosci. 2009; 12:1594–1600. [PubMed: 19915566]

17. Mitchell JF, Sundberg KA, Reynolds JH. Spatial attention decorrelates intrinsic activity fluctuations in macaque area V4. Neuron. 2009; 63:879–888. [PubMed: 19778515]

18. Pestilli F, Carrasco M, Heeger DJ, Gardner JL. Attentional enhancement via selection and pooling of early sensory responses in human visual cortex. Neuron. 2011; 72:832–846. [PubMed: 22153378]

19. Zenon A, Krauzlis RJ. Attention deficits without cortical neuronal deficits. Nature. 2012; 489:434–437. [PubMed: 22972195]

20. Bullier J, Henry GH. Ordinal position afferent input of neurons in monkey striate cortex. J. Comp. Neurol. 1980; 193:913–935. [PubMed: 6253535]

21. Chen Y, et al. Task difficulty modulates the activity of specific neuronal populations in primary visual cortex. Nature Neuroscience. 2008; 11:974–982. [PubMed: 18604204]

22. Luck SJ, Chelazzi L, Hillyard SA, Desimone R. Neural mechanisms of spatial selective attention in area V1, V2, V4 of macaque visual cortex. J. Neurophys. 1997; 77:24–42.

23. Motter BC. Focal attention produces spatially selective processing in visual cortical areas V1, V2, V4 in the presence of competing stimuli. J. Neurophysiology. 1993; 70:909–919. [PubMed: 8229178]

24. Yoshor D, Ghose GM, Bosking WH, Sun P, Maunsell JHR. Spatial attention does not strongly modulate neuronal responses in early human visual cortex. J. Neuroscience. 2007; 27:13205–13209. [PubMed: 18045914]

25. Usrey WM. The role of spike timing for thalamocortical processing. Current Opinion in Neurobiology. 2002; 12:411–417. [PubMed: 12139989]

26. Usrey WM, Alonso J-M, Reid RC. Synaptic interactions between thalamic inputs to simple cells in cat visual cortex. J. Neurosci. 2000; 20:5461–5467. [PubMed: 10884329]

27. Zohary E, Shadlen MN, Newsome WT. Correlated neuronal discharge rate and its implications for psychophysical performance. Nature. 1994; 370:140–143. [PubMed: 8022482]

28. Stratford KJ, Tarczy-Hornoch K, Martin KAC, Bannister NJ, Jack JJB. Excitatory synaptic inputs to spiny stellate cells in cat visual cortex. Nature. 1996; 382:258–261. [PubMed: 8717041]

29. Herrero JL, et al. Acetylcholine contributes through muscarinic receptors to attentional modulation in V1. Nature. 2008; 454:1110–1114. [PubMed: 18633352]

30. Disney AA, Aoki C, Hawken MJ. Gain modulation by nicotine in macaque V1. Neuron. 2007; 56:701–713. [PubMed: 18031686]

Methods References

31. Briggs F, Usrey WM. A fast reciprocal pathway between the lateral geniculate nucleus and visual cortex in the macaque monkey. J. Neurosci. 2007; 27:5431–5436. [PubMed: 17507565]

32. Briggs F, Usrey WM. Parallel processing in the corticogeniculate pathway of the macaque monkey. Neuron. 2009; 62:135–146. [PubMed: 19376073]

33. Skottun BC, et al. Classifying simple and complex cells on the basis of response modulation. Vision Res. 1991; 31:1079–1086. [PubMed: 1909826]

34. Brody CD. Slow covariations in neuronal resting potentials can lead to artefactual fast cross-correlations in their spike trains. J. Neurophysiology. 1998; 80:3345–3351. [PubMed: 9862930]
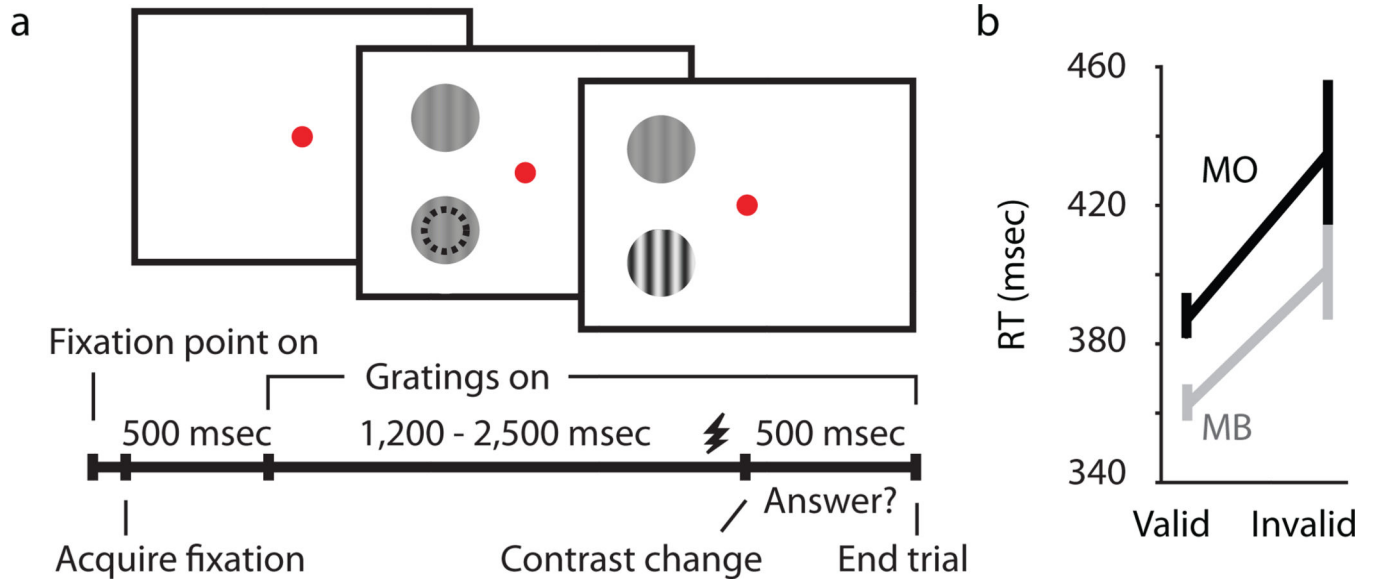
Figure 1.
Attention task and behavioral performance. (**a**) Illustration of the attention task including representative frames of the visual display for a validly cued trial where attention was directed by cue color toward the receptive field of the neuron. Dashed black circle represents the receptive field of the recorded neuron. The timeline for one trial is shown at bottom; LGN shock timing is indicated schematically just prior to the contrast change (shocks occured on 70% of trials). (**b**) Reaction time (RT) data for valid versus invalid trials for the two monkeys (Monkey B (MB), p=0.006; Monkey O (MO), p=0.046). Error bars represent SEMs.
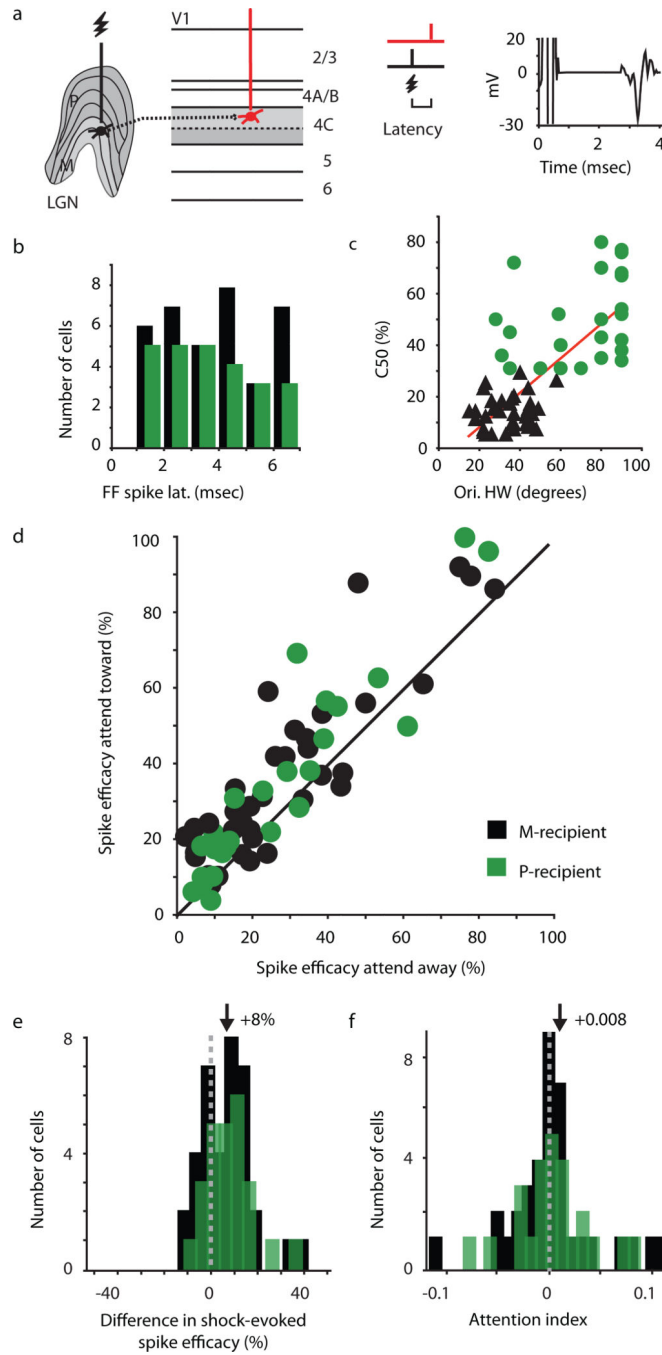
Figure 2.
Attentional modulation of thalamocortical synaptic efficacy. (**a**) Experimental set-up.
Electrical stimulation of presynaptic LGN neurons (black) leads to a postsynaptic response
in the simultaneously recorded TCR neuron (red). Shock-evoked postsynaptic spikes occur
at fixed latencies with little temporal jitter, as illustrated by trial-averaged waveform of a
representative TCR neuron (right). (**b**) Distribution of postsynaptic-response latencies for
M- and P-recipient neurons in black and green, respectively (mean latency: M-recipient
neurons = 3.4±0.3msec, P-recipient neurons = 3.1±0.4msec). (**c**) Relationship between C50

(contrast for half-maximum response) and orientation-tuning bandwidth (peak half-width, HW, at half height) for M- and P-recipient neurons ($R^2 = 0.52$). M-recipient neurons: C50 =13.8±1.1%, orientation HW = 34±1.8°. P-recipient neurons: C50 = 49.4±3.4%, orientation HW = 69±4.6°. (**d**) Percentage of shock-evoked postsynaptic spikes in attend-toward versus attend-away conditions. Black line represents unity. Average efficacy (percentage of shocks that evoke a postsynaptic response) for all TCRs: attend-toward = 36±3%, attend-away = 28±3%; M-recipient neurons: attend-toward = 37±4%, attend-away = 29±4%; P-recipient neurons: attend-toward = 35±5%, attend-away = 28±5%. (**e, f**) Distributions of differences in shock-evoked spike efficacy and attention index (AI) values for M- and P-recipient neurons (note difference in scales). AI values calculated from firing rate 850–1,200 msec following onset of grating stimulation. Dashed lines indicate zero and arrows indicate mean values (mean diff. spike efficacy M- and P-recipient TCRs = 8±2%; mean AI M-recipient = 0.008±0.007, P-recipient = 0.006±0.007).
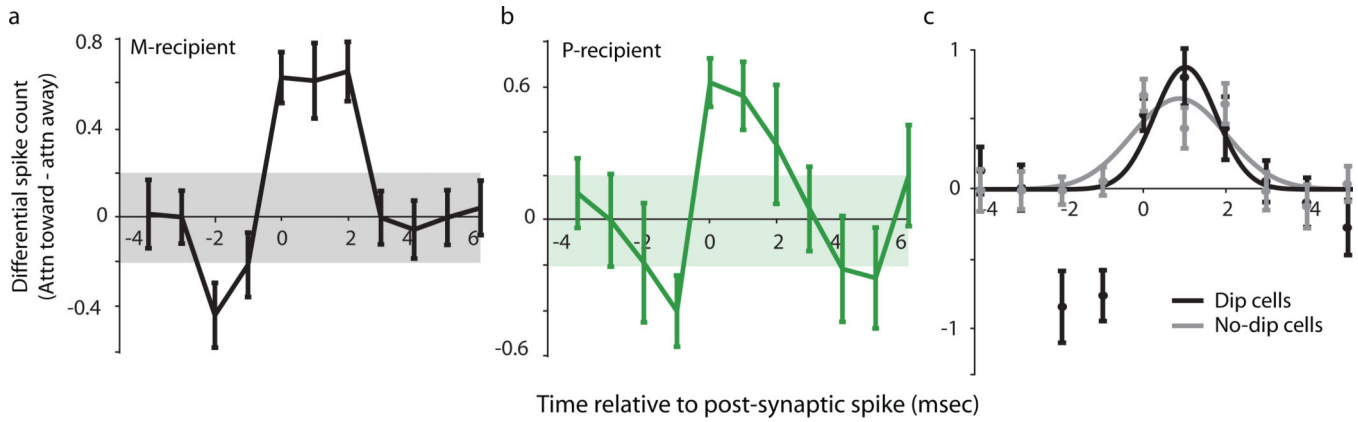
Figure 3.
Temporal precision of attentional enhancement of synaptic efficacy. Average differential spiking activity (attend-toward – attend-away) surrounding the time of the shock-evoked postsynaptic spike (occurring at time=0) for (**a**) M-recipient TCR neurons, and (**b**) P-recipient TCR neurons. Error bars represent SEMs; shaded regions represent 2 standard deviations above and below mean activity. (**c**) Average differential spiking activity of TCR neurons separated into groups on the basis of displaying early inhibition (Dip vs. No-dip cells). Error bars represent SEMs. Black and grey lines illustrate Gaussian fits to Dip and No-dip cell data. Width at half height for Dip cells = 1.75msec, for No-dip cells = 2.75msec.
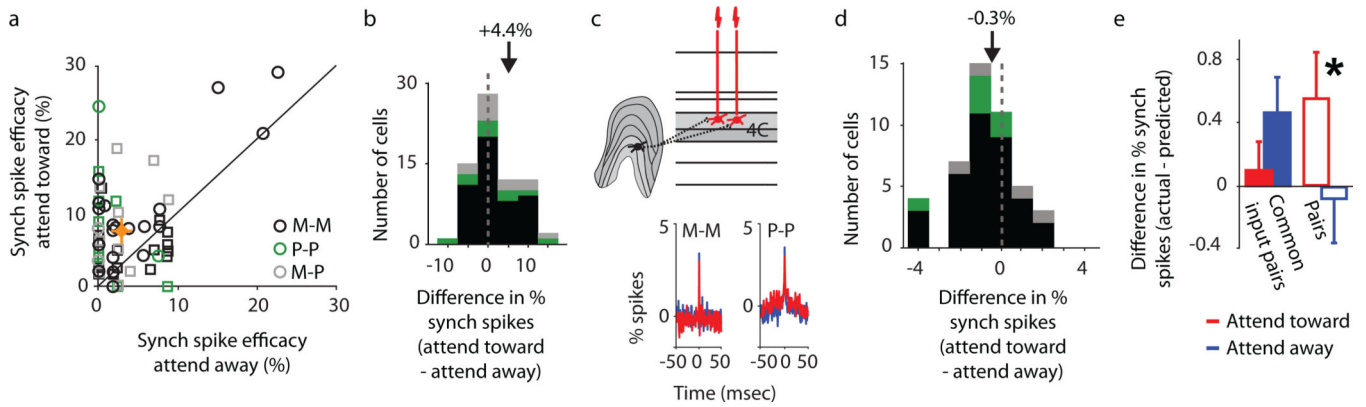
Figure 4.

Attentional modulation of synchronized spiking. (**a**) Percentage of synchronously evoked postsynaptic spikes across attention conditions for 71 pairs of simultaneously recorded M-M (black; n=48), P-P (green; n=11), M-P (grey; n=12) TCR pairs (circles represent TCR pairs; squares represent putative TCR pairs). Black line represents unity. Average synchronous-spiking efficacy across all pairs attend-toward condition = 7.6±0.8%, attend-away condition = 3.1±0.6% (orange diamond, crosshairs represent SEMs). (**b**) Distribution of attention-mediated differences in percentage of shock-evoked synchronous spikes. Color conventions as in **a**. Dashed line represents zero and arrow illustrates population mean (+4.4±0.7%). (**c**) Diagram illustrating a pair of TCR neurons receiving common presynaptic input and two examples of shuffle-corrected cross-correlograms for M-M recipient and P-P recipient pairs illustrating the occurrence of synchronous spikes (narrow peaks centered at time zero) and the influence of attention on the percentage of synchronous spikes in attend-toward (red) and attend-away (blue) conditions. (**d**) Distribution of attention-mediated differences in correlated spikes among pairs receiving common input (21 M-M, 2 P-P, and 2 M-P pairs). Conventions as in **b**. Mean difference in spikes in peak = −0.3±0.2%. (**e**) Difference between actual and predicted synchronous spikes for TCR pairs receiving common feedforward input (solid bars; n=25) and TCR pairs receiving independent input (open bars; n=46) across attention conditions. Error bars represent SEMs; asterisk indicates significant difference across attention conditions for TCR pairs receiving independent input (p = 0.02). Average actual – predicted values: common input TCR pairs, attend-toward = 0.1±0.2%, attend-away = 0.5±0.2%; independent input TCR pairs, attend-toward = 0.6±0.3%, attend-away = −0.1±0.3%.